Available online at www.sciencedirect.com
SCIENCE DIRECT
Polymer 46 (2005) 5860–5867
polymer
www.elsevier.com/locate/polymer

Processing and assessment of poly(butylene terephthalate) nanocomposites reinforced with oxidized single wall carbon nanotubes

G. Broza[a,*], M. Kwiatkowska[b,1], Z. Rosłaniec[b,1], K. Schulte[a]

[a]*Polymer Composites Group, Technical University Hamburg-Harburg, Denickestr. 15, D-21073 Hamburg, Germany*
[b]*Szczecin University of Technology, Institute of Materials Science and Engineering, Al. Piastöw 19, 70310 Szczecin, Poland*

Received 3 November 2004; received in revised form 11 May 2005; accepted 11 May 2005
Available online 14 June 2005

Abstract

Thermoplastic composites with carbon nanotubes (CNT) have a great potential as structural material because of their superior mechanical properties and ease of processing. The objective of this report is to evaluate the effect of oxidized single walled carbon nanotubes (oSWCNT) on the properties of poly(butylene terephthalate) (PBT) thermoplastic polymers, as a function of their weight content. The nanocomposites are obtained by introducing the oSWCNT into the reaction mixture whilst the synthesis of PBT. The polymers without and with carbon nanotubes were synthesised using an in situ polycondensation reaction process. Weight percentages ranging from 0.01 to 0.2 wt% of single walled nanotubes were dispersed in 1,4-butanediol (BD) by ultrasonication and ultrahigh speed stirring. After polycondensation the nanocomposites were extruded followed by injection moulding. The samples were characterised by thermal analysis, electron microscopy, dynamic-mechanical analysis, and tensile testing.

The addition of only a small amount of oSWCNT was enough to improve the thermo-mechanical properties of the nanocomposites. The Young's modulus, tensile strength, and strain to failure increased with increasing amount from 0.01 to 0.1 wt% of CNT in the PBT matrix. However, when the content of CNT was increased from 0.1 to 0.2 wt%, the strength and the strain of the nanocomposites decreased slightly.

Keywords: Nanocomposite; Carbon nanotube; Poly(butylene terephthalate)

1. Introduction

Besides their already good mechanical and physical properties combined with excellent processing conditions the properties of high polymers can further be enhanced by compounding with glass or carbon fibre fillers. The recently found carbon nanotubes have the potential to further improve the properties, especially when single walled carbon nanotubes (SWCNT) are used [1–4]. This mainly due to their high Young's modulus (~1 TPa) and strength (~1800 GPa) [5–7]. Their intrinsically high electrical conductivity together with the high aspect ratio (diameter ~1 nm, length up to few μm) enables electrical percolation and electrical conductivity at an extremely low volume content of nanotubes. This has been shown for thermosets [3] and recently also for thermoplastics [8,9]. The positive effect of nanotubes to polymer properties cannot only be derived directly from the CNT properties and their volume fraction, but also from their influence on morphology, crystalinity [10] and glass transition temperature [11–13]. Despite these promises, it has proved difficulties to exploit these impressive fundamental properties in experimental composites due to the need to disperse the individual nanotubes in the matrix, and to ensure sufficient interfacial stress transfer between nanotubes and matrix [14]. However, the outstanding mechanical properties of SWCNT will be of little value unless they cannot properly be incorporated into a matrix. The main issue in the production of carbon nanotube reinforced polymers is to avoid the agglomeration of nanotubes in the polymer matrix [8,9]. All of the dispersing experiments up to now were based on the same principle, which was a disagglomeration and, taking advantage of a low matrix viscosity.

Three methods were commonly used to produce

* Corresponding author. Tel.: +49 40 428 78 3496; fax: +49 40 42878 2002.
E-mail addresses: broza@tuhh.de (G. Broza), zbigniew.roslaniec@ps.pl (Z. Rosłaniec).
[1] Fax: +48 91 4340558.

0032-3861/$ - see front matter © 2005 Elsevier Ltd. All rights reserved.
doi:10.1016/j.polymer.2005.05.073

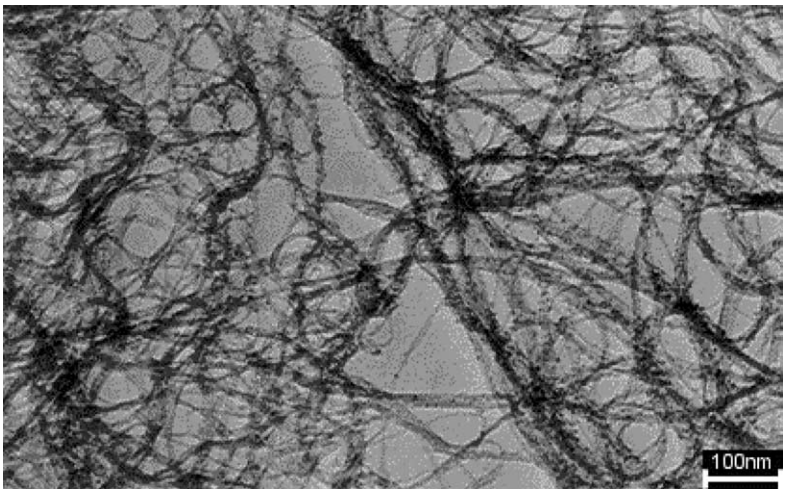

Fig. 1. TEM image of the oxidized single walled nanotubes, oSWCNT.

polymer/CNT nanocomposites: (i) solution mixing [15–17], (ii) melt blending [18,19], and (iii) direct polymerisation in the presence of nanotubes [20–22]. In the present paper, we describe a method to produce poly(butylene terephtalate) (PBT) nanocomposites with oxidized single wall carbon nanotubes (oSWCNT) by using an in situ polycondensation process, first introduced for multiblock copoly(ether-*b*-ester)s based on semicrystalline poly-(butylene terephtalate) blocks (PBT) and amorphous nanocrystalline oxytetramethylene blocks (PTMO) [23]. This approach was aimed to easy disperse of carbon nanotubes within the matrix during the reaction process, preserving their structure and integrity and enabling an effective load transfer. The objective of the study was to evaluate the effect of oxidised single walled carbon nanotubes in PBT as a function of their weight fraction. Ultrasound processing and stirring of one of the monomers of polycondensation reaction, namely 1,4-butanediol (BD), has been chosen as most promising. However, while successful in dispersing with sonication, the technique may cause a short cut of CNTs due to local high energy input.

2. Experimental

2.1. Materials

The reagents were purchased from BASF, Germany (1,4-butanediol, BD) and Du Pont, USA (dimethyl terephthalate, DMT). Commercially available solvents were purified by distillation. Common reagents were used without further purification.

The oxidized single walled carbon nanotubes (oSWCNT) used in this study were ready supplied by CNI Technology Co., TX, USA, synthesised by the HIPCO method [24]. Carbon nanotubes can be oxidized by means of two methods, which are gas phase and liquid phase oxidation [25]. Gas phase oxidation is normally performed by heating the nanotubes (up to ca. 873 K) in oxidative atmosphere (e.g. air). However, liquid phase chemical oxidation has advantages over the gas phase process. It results in tubes, which can easier be handled and the reaction degree can better controlled. The liquid phase oxidation is most commonly being performed boiling nanotubes in a mixture of sulphuric and nitric acids. This oxidation procedure results in:

- purification of the nanotube soot via etching away the less stable carbon impurities (amorphous carbon etc.),
- it leads to local damage which can result in cutting (shortening) of the tubes and might destroy the tube caps (opening),
- sidewall functionalisation on the nanotubes via formation of hydroxyl groups (–OH).

Well separated and shortened nanotubes should be easier to uniformly distribute in the matrix and are expected not to show an as strong tendency to reagglomerate during processing.

The diameter of the oSWCNT was 0.7–1.2 nm with a length of few μm. A TEM image of the oSWCNT is shown in Fig. 1.

2.2. Processing of PBT with oSWCNT nanocomposites

Processing of nanocomposites via in situ polycondensation of PBT is explained in the following on the example of 0.1 wt% 245 g of 1,4-butanediol and 0.3 g of oSWCNT were stirred for 5 min at 20.000 rpm, followed by degassing in a vacuum oven at 50 °C. In a second step, the dispersion was sonicated for 5 min at room temperature (SONOPLUS-Homogenissator HD 2200 with a titanium sonotrode (Bandelin Electronic GmbH, Berlin, Germany). The first step and the second step were repeated six times. Finally,

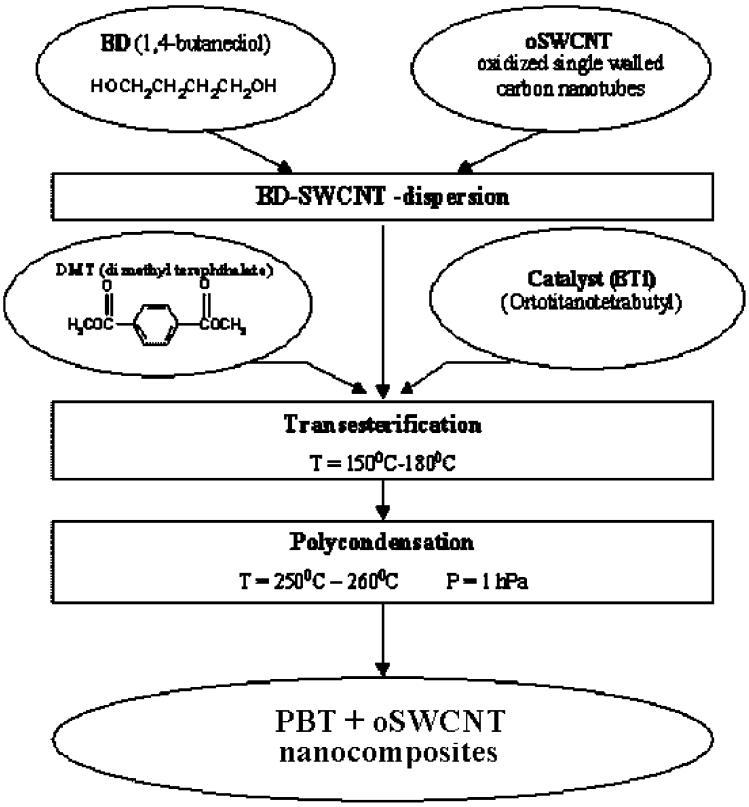

Fig. 2. Schematic illustration of the PBT+oSWCNT composites processing.

the system has been degassed again for 30 min at 50 °C in the vacuum oven.

In a steel reactor of 1 dm^3 volume (Autoclave Eng., Inc., USA), 270 g of dimethyl terephthalate (DMT) (1.4 mol) and 60 mg (2.1×10^{-4} mol) of tetrabutyl orto-titane (TiBu) were mixed. oSWCNT-BD was slowly added to this mixture and mechanically stirred to obtain a homogeneous dispersion. Then this mixture was slowly heated for 1 h to 180 °C under a steady stream of N_2 gas. Next, the temperature was raised to 225 °C and hold for 2 h. During this period, continuous generation of distilled BD and methanol, in the relation of the theoretical amount, was observed. Finally, the system was heated for 2 h at 260 °C, during which the pressure decreased step by step down to 1 hPa. The progress of reaction was controlled on the basis of the amount of distilled BD and on the increasing momentum (revolutions per minute, rpm) of the stirrer. A schematic illustration of the composite synthesis is shown in Fig. 2.

The polymer produced was extruded from the reactor by compressed nitrogen and cooled to room temperature, repeatedly washed in water, and dried in vacuum at 60 °C for 1 day, and granulated. Neat PBT and four different PBT nanocomposites with different wt% of oSWCNT were produced and are presented in Table 1 together with the label assigned to each composite.

Table 1
Nomenclature, CNT weight content, limiting viscosity number [η], and legend of the studied materials

Sample	Weight content of SWCNT (%)	η (dl g^{-1})
PBT	0	0.96
PBT/SW01	0.01	0.96
PBT/SW05	0.05	0.95
PBT/SW1	0.1	0.92
PBT/SW2	0.2	0.90

[η] = limiting viscosity number was measured using an Ubbelohde 1 capillary viscometer. The polymers were dissolved in phenol–trichlorethylene solution (1:1 vol/vol), and measurements were done at 30 °C. CNTs have been separated from PBT/CNT solution by filtration.

2.3. Injection moulding

For testing mechanical properties hour glass shoped specimens were injection moulded, using a Baby Plast, Model 6/10 (Cronoplast S.L. Comp.) injection moulding machine. The processing conditions were kept constant for

Table 2
Processing conditions used in injection moulding

Injection pressure (bar)	25
Hold pressure (bar)	20
Hold time (s)	6
Cooling time (s)	20
Mould temperature (°C)	40–60
Melt temperature (°C)	240–250

Note: the pressures are those of the hydraulic system.

Table 3
Thermal properties of PBT with oSWCNT

Sample	$T_{m'}$ (°C)	T_{c1} (°C)	T_{c2} (°C)	T_{c3} (°C)	$T_{m''}$ (°C)	ρ (g/cm^3)	ΔH_m (J/g)	$X_{c(tot)}$ (%)
PBT	222	186.4	193.5	197.3	222	1.30635	61.7	44
PBT/SW01	224	188.6	197.5	200.7	223	1.30628	56.9	40
PBT/SW05	224	190.1	198.9	202.9	223	1.30725	57.6	41
PBT/SW1	224	192.9	200.8	205.1	223	1.31186	57.3	41
PBT/SW2	227	190.7	199.8	205.5	223	1.30532	49.3	35

Note: $T_{m'}$, melting peak separature of 1st heating; $T_{m''}$, melting peak separature of 2nd heating; T_{c1}, crystallisation extrapolated onset temperature; T_{c2}, crystallisation peak temperature; T_{c3}, crystallisation extrapolated end temperature.

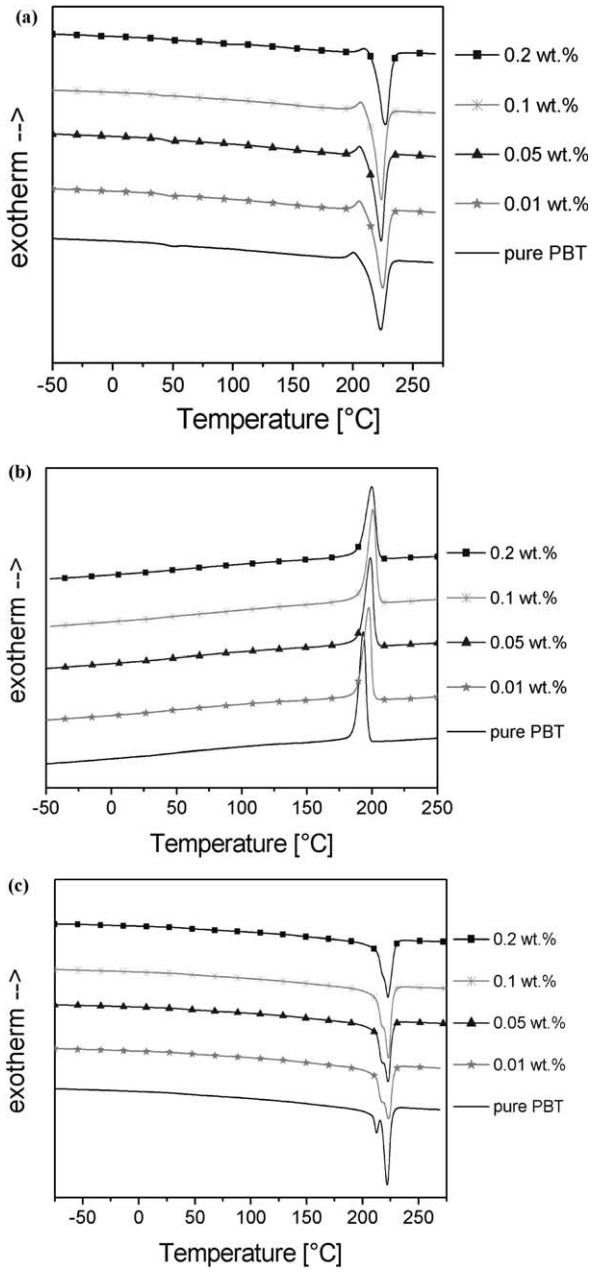

Fig. 3. (a) DSC curves of 1st heating of PBT and PBT + oSWCNT. (b) Non-isothermal crystallisation of PBT and PBT + oSWCNT. (c) DSC curves of 2nd heating of PBT and PBT + oSWCNT.

the different nanocomposites including the unreinforced PBT.

The parameters of injection moulding are displayed in Table 2.

2.4. Characterisation

Non-isothermal crystallization analysis was performed by means of a differential scanning calorimeter (DSC) (SEICO (Seico Instruments, Japan)). The standard procedure performed was: samples of about 15 mg were heated from −50 to +260 °C at a scan rate of 10 °C/min and held for 10 min in order to eliminate any thermal history of the material. Subsequently, the samples were cooled to 50 °C using scan rates of 10 °C/min. In order to observe, the melting peak after crystallization, the samples were reheated to +260 °C at a heating rate of 10 °C/min under a N_2 flow. Mechanical tensile properties were investigated on a tensile test machine (Zwick GmbH, Germany) with a crosshead speed of 5 mm/min. Five specimens were taken for each material.

Dynamic mechanical thermal analysis (DMTA) measurements were carried out on a Qualimeter EXPLEOR 500 N (Gabo Comp., Germany) in the tensile mode. The materials were cut into strips with lengths of 40 mm and thickness of 2.5 mm. The samples were heat treated at +120 °C for 4 h and were then stored in a desiccator. This was done to remove any humidity effects prior to testing. Tests were performed at a frequency of 10 Hz between −120 and +180 °C with a ramp of 3 °C/min.

The characterization of the fracture surface of the samples was investigated after slight gold sputtering, using a field emission scanning electron microscope (SEM FEG) Model LEO 1530 (Leo Electron Microscopy Ltd, Zeiss, Oberkochem, Germany).

For transmission electron microscope (TEM) investigation ultra thin cuts were made on a Leica Ultracut-E cryo microtome at a temperature of −80 °C with a diamond knife. The thickness was about 60 nm. The TEM elastic bright field images were taken on a Philips EM 402, operating at 100 kV.

Shore D hardness were tested according to DIN 53505 using a test maschine Zwick 3100 Shore D (Zwick GmbH, Germany).

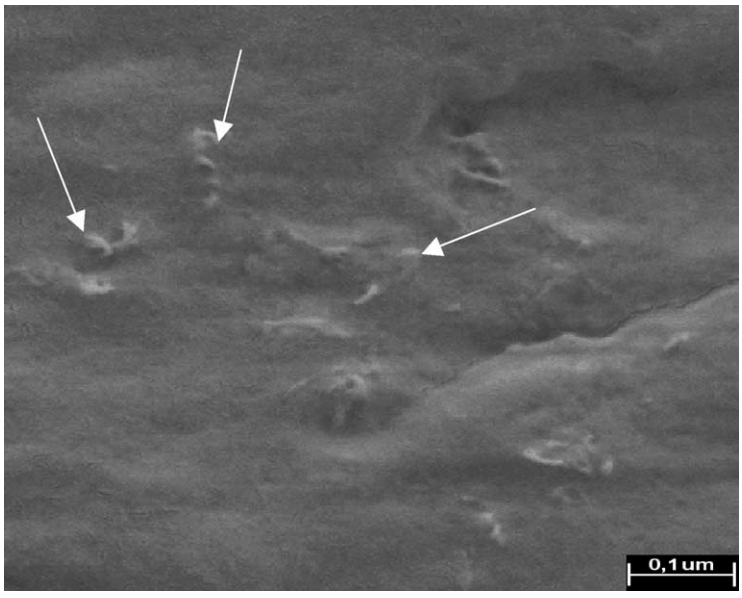

Fig. 4. SEM-FEG micrographs of the cryogenic fractured surface of PBT with 0.1 wt% oSWCNT.

3. Results and discussion

3.1. Dispersion of single walled carbon nanotubes in BD-system

The two-stage polycondensation method in molten state was applied to obtain poly(buthylene terephthalate) polymers with oSWCNT dispersed in BD and added to the reaction mixture. The essential element of obtaining the composites in such a way was the complete dispersion of nanotubes in BD just before starting the synthesis.

However, successful in dispersing, this technique causes reduction in length of CNTS due to oxidation process an additional step to the process, which is disagglomeration in the solvent 1,4-butanediol.

3.2. Thermal properties

From the DSC-tests crystallisation and melting thermograms were recorded during the heating and cooling processes for anisothermal measurement. From these thermograms, the thermal parameters of melting temperature (T_m), crystallisation temperature (T_{c1}, T_{c2}, T_{c3}), melting enthalpy (ΔH_m), crystallisation enthalpy (ΔH_c), percentage of crystallinity ($X_{c(tot)}$) were obtained and density are summarized in Table 3. The $X_{c(tot)}$) was calculated from the melting enthalpy ΔH_m (J g^{-1}) to

$$X_{c(tot)} = \frac{\Delta H_m}{\Delta H_f} \times 100$$

with $\Delta H_f = 140$ J g^{-1}, the theoretical value of enthalpy for a 100% crystalline poly(buthylene terephthalate) homopolymer [26]. The decrease of ΔH_m with increasing nanotube concentration can be directly attributed to the reduction of the PBT concentration in the nanocomposites. The detailed DSC curves are presented in Fig. 3(a)–(c). The melting point of 1st heating (Fig. 3(a)) seems not to be affected by presence of the fillers. There is no evidence to assume that the crystallite size has changed. However, carbon nanotubes accelerate crystallisation during cooling and in consequence, the crystallisation peaks of the DSC curves shift to higher temperatures (about +5 °C higher when compared neat PBT (Fig. 3(b)). With increasing CNT concentration (to 0.1 wt% oSWCNT), the T_c also increases, suggesting that interactions between the CNT and the matrix occur. This kind of crystallisation was also observed in nanofiber-reinforced thermoplastic composite systems [27]. However, the 2nd heating shows some differences. (Fig. 3(c)). The nanocomposites have a broader melting peak when compared to the pure PBT matrix. This difference may suggest that nanocomposites possess less perfect crystals or a broader distribution of crystal size than the neat PBT. Besides, double melting was observed only in neat PBT and interpreted in terms of reorganisation processes occurring during the 2nd heating [28]. In the samples with oSWCNT, the low-temperature peak was barely visible and diminished with increasing CNT content. The results confirm that the addition of a low concentration of nanotubes enhances the nucleation process on PBT crystallisation.

3.3. Morphology

SEM-FEG (Field Emission Scanning Electron Microscope) micrograph shows an cryogenic fractured surface of a PBT/CNT nanocomposite prepared with 0.1 wt% oSWCNT (Fig. 4). For the PBT/SWCNT nanocomposite, if a good dispersion and break down of the nanotubes ropes is attained by purification (oxidized SWCNT), the

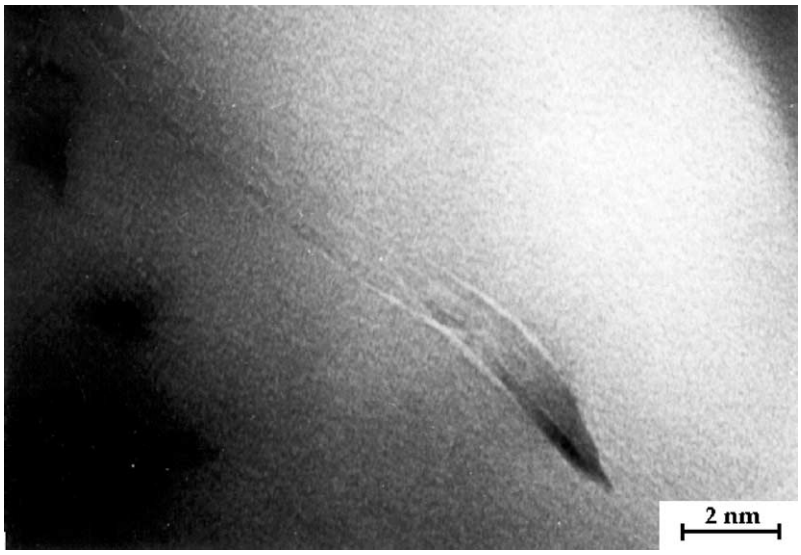

Fig. 5. TEM micrograph of a single oSWCNT in the PBT matrix.

Table 4
The mechanical properties of the PBT/oSWCNT nanocomposites

Sample	Young's modulus (MPa)	Tensile strength R_m (MPa)	Fracture strain ε (%)	Hardness Shore D
PBT	2240	38	4.0	75.2
PBT/SW01	2325	43	11.4	76.1
PBT/SW05	2360	44	11.5	78.1
PBT/SW1	2555	49	7.0	77.7
PBT/SW2	2650	43	3.2	77.1

individual nanotubes will not be observable with SEM-FEG, due to their small size and the level of magnification achieved. In fact, SEM-FEG observation of the cryogenic fracture surfaces of these nanocomposites did not show any considerable amount of nanotubes. Only some dispersal CNT bundles can be observed (arrows). There is no clear evidence of agglomeration. The TEM micrograph shows a single oSWCNT in the PBT matrix (Fig. 5).

3.4. Mechanical and dynamical properties

All the samples were characterized according to their mechanical and dynamical properties. For ease of comparison, Figs. 6–8 depict, therefore, the normalised that means divided (by the neat matrix values) Young's modulus, tensile strength and fracture stress, respectively. In comparison to the neat PBT tensile test results showed that nanotubes dispersed via in situ polycondensation in PBT improve tensile strength and at the same time the tensile strain. It can be observed that with an increase from 0.01 to 0.1 wt% oSWCNT (sample PBT/SW01 and PBT/SW1) concentration the Young's modulus, tensile strength and strain to failure increase. This may be attributed to a better performance of the carbon nanotubes when incorporated in the PBT. On the other hand, the tensile strength and strain to failure are reduced by the incorporation of 0.2 wt% oSWCNT (sample PBT/SW2). It may be caused by disturbance of PBT crystallization in this sample. In comparison to the nanocomposites with up to 0.1 wt%

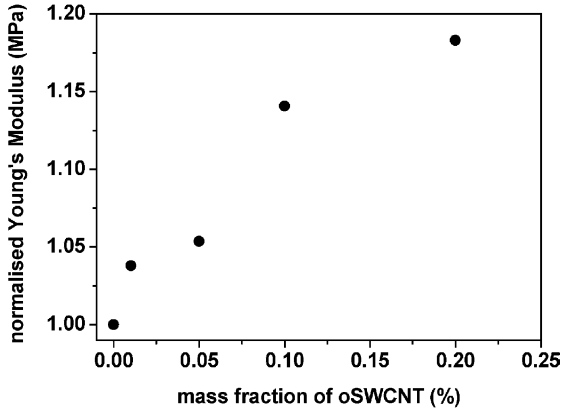

Fig. 6. Normalised Young's modulus plotted versus mass fraction of oSWCNT.

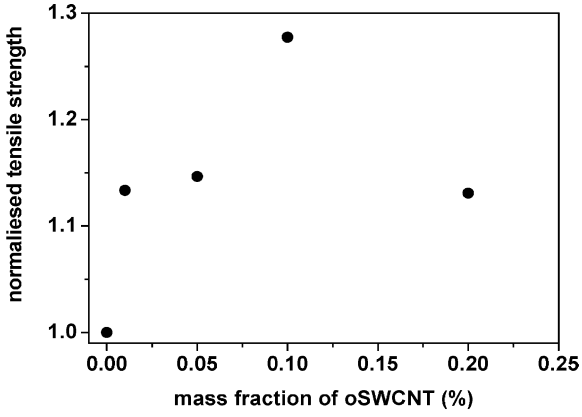

Fig. 7. Normalised tensile strength plotted versus mass fraction of oSWCNT.

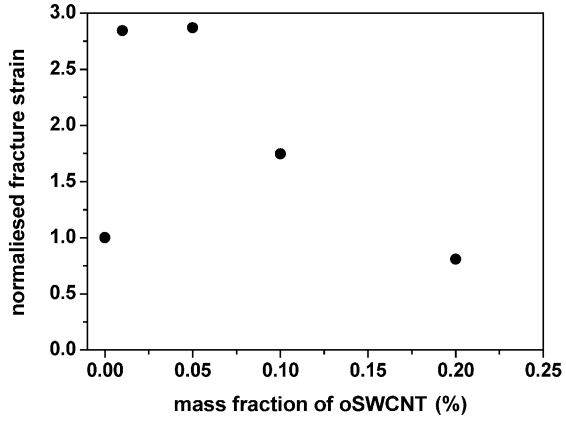

Fig. 8. Normalised fracture strain plotted versus mass fraction of oSWCNT.

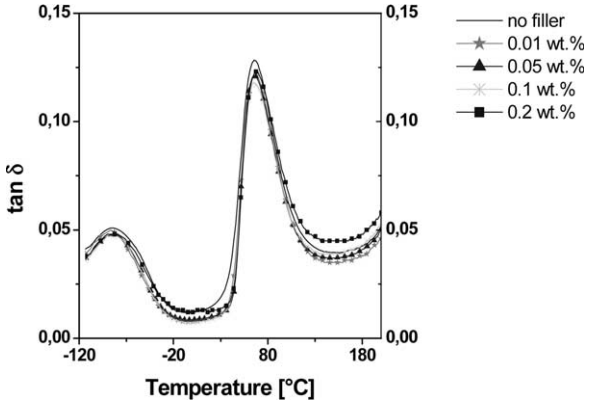

Fig. 10. Temperature dependent tan δ versus for PBT and PBT modified by oSWCNT.

oSWCNT where the crystallinity $X_{c(tot)}$ increases, the crystallinity of PBT with 0.2 wt% oSWCNT concentration decreases instantly (Table 3). A similar trend was observed for the Shore D hardness of the nanocomposites (compare Table 4). The Shore D hardness of the nanocomposites decreased beyond the incorporation of 0.1 wt% oSWCNT.

Table 4 lists the average values for Young's modulus, tensile strength, fracture strain, and Shore D hardness as a function of oSWCNT content in the PBT matrix.

The dynamic mechanical properties of the neat matrix and polymer nanocomposites were studied by DMTA. Fig. 9 shows the temperature dependent storage modulus E' and loss modulus E'' of PBT and various nanocomposites. In all nanocomposites the incorporation of oSWCNT causes a measurable increase in the stiffness. The storage modulus E' of PBT is increased by the stiffening effect of the nanotubes, which is particularly significant at temperatures between $T = -120$ and $+55$ °C, (which is below T_g of PBT). This is a hint that the reinforcement effect of CNT's is mainly active in the amorphous phase, which also leads to the suggestion that the nanotubes are mainly present in this phase.

Compared to carbon nanotube/PMMA composites [18], the stiffening effect is less significant for PBT with oSWCNT nanocomposites. Certainly, PMMA is an amorphous polymer whereas PBT is semicrystalline. In comparison with amorphous polymers, the crystallites in PBT already impart a high modulus and hence the nanotubes do not induce a dramatic increase in stiffness of the semicrystalline matrix. In fact, some authors did predict that a larger relative improvement in the modulus would be observed if an amorphous PMMA polymer matrix [19] was used in place of crystalline PVA [17].

Above T_g of PBT a slight increase in E' can be observed, this leads to the suggestion of a nucleation effect of the CNT's for the crystalline phase of PBT. This result could be expected as a similar behaviour was observed in [10] for PP. The maximum of the loss modulus E'' taken as glass

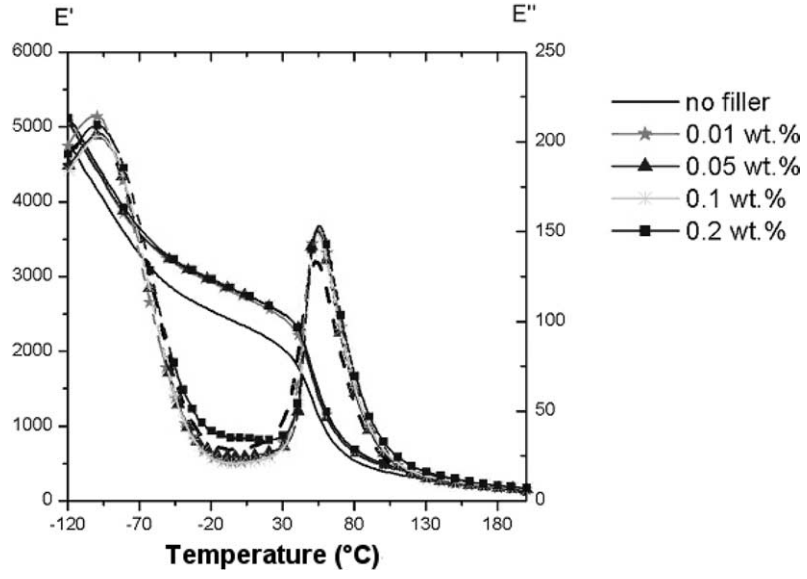

Fig. 9. Temperature dependent storage modulus E' and loss modulus E'' of PBT and the various nanocomposites.

relaxation. In Fig. 10 is plotted tan δ versus temperature for PBT modified by oSWCNT. The tan δ peak of the composite shows some broadening and moves to a slightly higher temperature. The maximum of the tan δ is commonly taken as the glass transition temperature (T_g), and is the same for all samples.

4. Conclusion

Oxidized SWCNT are incorporated in poly(butylene terephthalate) thermoplastic polymers in order to assess the effectiveness of the polycondensations process. The oSWCNT were nicely dispersed with a minor trend for agglomeration.

The effects of different oSWCNTs concentrations on the crystallisation of PBT were analysed by DSC. The nucleation and crystal growth is accelerated in PBT and this effect is more evident at the lower oSWCNT content (up to 0.1 wt%).

We found that a small amount of CNT was enough to improve the mechanical properties of the PBT matrix. In the present work, it has been shown that PBT/oSWCNT thermoplastic nanocomposites can be produced with tensile modulus, tensile strength and fracture strains considerably higher than those for the neat PBT. The ultimate tensile strength and strain to failure of the PBT/oSWCNT increased with the addition of carbon nanotubes up to a critical content of 0.1 wt% and then decreased. However, the initial Young's modulus increased with increasing amount of oSWCNT in the PBT matrix. In comparison to the neat PBT tensile test results of PBT/SWCNT nanocomposites showed improve tensile strength and at the same time the tensile strain.

In conclusion, in situ polycondensation of poly(butylene terephthalate) with oxidized single wall carbon nanotubes offers a simple and effective means to produce nanocomposites. The nanotubes are well dispersed in the polymer matrix (up to 0.1 wt% oSWCNT). Further studies of the relationship between the mechanical properties and the different molecular weight of the matrix will be performed.

Acknowledgements

The European Commision (Scientific Network: 'Carbon Nanotubes for Future Industrial Composites: theoretical potential versus immediate application (CNT-Net)'; Contract No.: G5RT-CT-2001-050206) are gratefully acknowledged for financial support.

References

[1] Lourie O, Wagner HD. Appl Phys Lett 1998;73(24):3527–9.
[2] Lourie O, Wagner HD. J Mater Res 1998;13(9):2418–22.
[3] Sandler J, Shaffer MSP, Prasse T, Bauhofer W, Schulte K, Windle AH. Polymer 1999;40:5967–71.
[4] Lourie O, Wagner HD. Phys Rev Lett 1998;81(8):1638–41.
[5] Calvert P. Nature 1999;399:210–1.
[6] Salvetat JP, Briggs GAD, Bonard JM, Bacsa RR, Kulik AJ, Stöckli T, et al. Phys Rev Lett 1999;82(5):944–7.
[7] Subramoney S. Adv Mater 1998;10(15):1157–71.
[8] Pötschke P, Dudkin SM, Alig I. Polymer 2002;44:5023.
[9] Gong X, Liu J, Baskaran S, Voise RD, Young JS. Chem Mater 2002; 12:1049.
[10] Sandler J, Broza G, Nolte M, Schulte K, Lam YM, Shaffer MSP. J Macromol Sci, Part B: Phys 2003;B42:3–4.
[11] Gojny FH, Schulte K. Comput Sci Technol 2004;64:2303.
[12] Chungui Z, Lijun J, Huiju L, Guangjun H, Shimin Z, Mingshu Y, et al. J Solid State Chem 2004;177:4394–8.
[13] Hao K, Chao G, Deyue Y. Macromolecules 2004;37:4022–30.
[14] Barrau S, Demont P, Peigney A, Laurent C, Lacabanne C. Macromolecules 2003;36:3187.
[15] Lamy de la Chapelle M, Stephan C, Nguyen TP, Lefrant S, Journet C, Bernier P, et al. Synth Met 1999;103:2510.
[16] Stephan C, Nguyen TP, de la Chapelle ML, Lefrant S, Jourent C, Bernier P. Synth Met 2000;108:139.
[17] Shaffer MSP, Windle AH. Adv Mater 1999;11:937.
[18] Haggenmueller R, Gommans HH, Rinzler AG, Fischer JE, Winey KI. Chem Phys Lett 2000;330:219–25.
[19] Zhaoxia J, Pramoda KP, Guoqin X, Suat HG. Chem Phys Lett 2001; 337:43–7.
[20] Jia ZJ, Wang ZY, Xu CL, Liang J, Wie BQ, Wu DH, Zhu SW. Mater Sci Eng 1999;A271:395.
[21] Hao K, Chao G, Deyue Y. J Am Chem Soc 2004;126:412–3.
[22] Shuhui Q, Dongqi Q, Warren TF, Daniel ER, Jose EH. J Am Chem Soc 2004;126:170–6.
[23] Roslaniec Z, Broza G, Schulte K. Compos Interfaces 2003;10(1): 95–102.
[24] Nikolaev P, Bronikowski MJ, Kelley BR, Rohmund F, Colbert DT, Smith KA, et al. Chem Phys Lett 1999;313:91–7.
[25] Shaffer MSP, Windle AH. Carbon 1998;36:1603.
[26] Illers KH. Colloid Polym Sci 1980;258:117–24.
[27] Lozano K, Barrera EV. J Appl Polym Sci 2001;79(1):125.
[28] Hobbs SY, Pratt CF. Polymer 1975;16:462–4.